Innovative Infrastructure Solutions (2024) 9:184
https://doi.org/10.1007/s41062-024-01502-9

TECHNICAL PAPER

Impact of diffraction on screening of dynamic compaction waves with barriers

N. Fathi Afshar[1] · A. Hamidi[1] · Gh. Tavakoli Mehrjardi[1]

Received: 31 January 2023 / Accepted: 17 April 2024 / Published online: 7 May 2024

Abstract
As the dynamic compaction operation is accompanied by heavy weights and hard tamping, its induced ground vibrations can cause the unfavourable effects on nearby pipelines and buildings, ranging from annoyance to structural damage. Therefore studying the performance of barriers is inevitable. The majority of these vibrations spreads as of surface (Rayleigh) waves. By spreading out the generated surface waves, wave barriers can be a successful way to minimize these effects. Based on this and due to the lack of previous field studies on wave barriers in dynamic compaction, conducting practical tests and direct measurements of wave characteristics such as peak particle velocity are considered urgent needs by the engineering community in order to obtain wave barrier design solutions. The effectiveness of open trenches, empty holes, and trenches filled with geofoam in reducing vibrations brought on by dynamic compaction was investigated in an experimental field investigation. The dimensions of 10×12 m are deemed big enough within the context of our study area to capture the pertinent characteristics and phenomena related to dynamic compaction. To assess the isolation efficiency, key parameters, including the barrier geometries, and their locations relative to the vibration source were examined. The Larger barrier dimensions and the closer proximity of barrier to the vibration source the better screening effects. The experimental results showed that for the applied range of dynamic compaction energy (6 t.m), open trench barriers reduced peak particle velocity in vertical direction by 50% and geofoam-filled barriers reduced it by 20%, proving a good contribution in mitigation of the aftereffects in terms of induced vibrations. Moreover, void holes provided the least protection with about a 12% decrease in the energy transferred. The results of these experimental field studies can be useful for design purposes.

Keywords Dynamic compaction · Peak particle velocity · Physical modelling · Wave barrier · Wave diffraction

Introduction

There are several ground-borne vibrations which can be induced by the machine foundations, high-speed trains, blast, rockfall and dynamic compaction dynamic. Most such vibrations transfer to the ground surface, and propagate in the form of surface waves which can travel for long distances. Ground-borne vibrations have the potential to upset nearby residential areas and may also have an impact on the functionality of delicate machinery. One of the most crucial aspects of vibration intensity, peak particle velocity, may be measured directly or using prediction models. This metric essentially serves as a benchmark for assessing the negative consequences of waves that propagate from the vibration source [1–4]. Wave barriers in the ground are generally used to reduce the aftereffects of induced vibrations. The geometry, location, and composition of a wave barrier will influence its performance. Wave barriers can be in the form of open trenches, in-filled trenches, sheet-pile walls, and the rows of solid or hollow piles (empty holes). Several analytical and numerical studies, as well as a few experimental studies surveyed the applicability of wave barriers for vibration isolation (known as vibration screening) to improve understanding of vibration scattering. By placing open trenches close to a wave source (known as active isolation) or next to an item like a machine or building that has to be protected (known as passive isolation), Woods [5] carried

✉ Gh. Tavakoli Mehrjardi
ghtavakoli@khu.ac.ir

N. Fathi Afshar
fathiafshar@yahoo.com

A. Hamidi
hamidi@khu.ac.ir

[1] Department of Civil Engineering, Faculty of Engineering, Kharazmi University, Tehran, Iran

out a series of scaled field tests on vibration isolation. Based on the data, Woods [5] provided recommendations for the size of open trenches to achieve a drop in ground amplitude equal to or higher than 75%. Better vibration reduction efficiency can be obtained using empty (open) trenches compared to in-filled trenches having the same geometrical and mechanical features [6–13]. To avoid instability associated with open trenches, the vertical edges of the barrier can be supported with concrete elements [14]. A similar beneficial stabilizing effect can be obtained using in-filled trenches, where the fill material provides larger elastic moduli values than the surrounding soil [15, 16]. Vibration reduction similar to that of in-filled vertical barriers was observed with the use of a sheet-pile wall or a row of piles [17–19]. It is possible to use weaker materials (smaller elastic parameters), such as geofoam, water, and bentonite as a filler [8–11, 16, 20–25].

Baker [26] and Ahmad et al. [27] conducted a series of field model tests to study the effectiveness of barriers made of bentonite (a soft barrier), and concrete (a stiff barrier) installed either close to or at a distance from the source of disturbance. They made comparisons between the experimental results and numerical findings from the literature that had been produced using the boundary element method (BEM) and empirical design equations created by Ahmad and Al-Hussain [28]. They discovered that compared to active isolation, passive isolation benefited more from the obstacles. Moreover, the bentonite barriers yielded slightly higher amplitude reduction ratios ($\overline{A}_r$) than the concrete barriers. The empirical formula compared reasonably well with the field test results, as well as with other published experimental data.

Beyond wave barriers technique, other researchers proposed an approach in the form of active wave generator for ground surface vibration reduction that are comparable to classic, and innovative vibration mitigation techniques [29]. The efficiency of approach was verified for harmonic excitation and impact loads at points located on the ground surface or below it.

Numerical models, which are more developed compared to the experimental studies, are efficient tools for investigating wave propagation problems. The finite element method (FEM) and boundary element method BEM were widely used in wave barrier simulations. Haupt [30], El Naggar and Chehab [31], Andersen and Nielsen [15], Beskos et al.[32], Ahmad and Al-Hussaini [29, 33–35], Al-Hussaini and Ahmad (1991 and 1996), Al-Hussaini et al.[29], Saika [37, 38], Bose et al. [39], Yao et al. [40] and Qiu [41] carried out numerical modelling to interpret the behaviour of open and infill wave barriers to reduce ground-borne vibrations. Saika [37, 38] showed that the isolation efficiency of open and in-filled trench barriers were largely governed by the impedance ratio (IR) of in-fill material in which IR is the ratio of impedance value (density × Rayleigh wave velocity) of the barrier to that of the surrounding soil. A reduction in IR was observed to boost the efficiency of isolation. Saika discovered that an in-filled trench had efficacy equivalent to an open trench with identical shape within an IR range of 0.08 to 0.17.

It should also be mentioned that some novel approaches, have been made to improve the estimation of PPV by automated intelligent hybrid computing methods, especially in blasting operations [42–44].

The studies mentioned above indicate that wave barriers can be used to effectively screen ground-borne vibrations. However, as a first limitation of these studies, most of them focused on harmonic waves and paid little attention to waves produced by impact loads such as dynamic compaction. As the second limitation, the fewer investigations performed about using wave barriers in dynamic compaction are generally based on numerical models and not according to the field measurements.

Therefore, it is important to examine the application of suggested protective measures and their effectiveness for vibration isolation in non-harmonic heavy excitation like dynamic compaction due to the lack of efficient solutions to mitigate the side effects of dynamic compaction operations. Furthermore, as the third limitation of previous studies, in dynamic compaction, wavelength is not a constant parameter like harmonic waves, and it was felt that a more appropriate parameter is needed to normalize the dimensional parameters of this operation.

The current investigations were carried out in light of the above and the need for a manual for the design of wave barriers in dynamic compaction operations. The present experimental investigation looked at the efficiency of several wave barriers (void holes, geofoam-filled trenches, and empty trenches) confronting waves that propagated owing to dynamic compaction and looked into the function of contributing elements. Finally, the effect of diffraction on efficiency of trenches and hole barriers has been precisely investigated.

Testing materials

Sub-soils

The test site was a flat open area located in the city of Mahdasht in Alborz province of Iran (Fig. 1). The selected area was 10×12 m^2 in plan. Based on investigation up to a depth of 10 m, the native soil was classified as sandy clay (CL) based on the Unified Soil Classification System (ASTM D2487-11), with a relative compaction of more than 85%. The effective depth of dynamic compaction used in the current study was 1–1.5 m; thus, the upper 2-m thickness layer of the native soil was replaced with coarse-grained sandy

Fig. 1 Vicinity map of study area

soil, which was classified as SC in the Unified Soil Classification System. This soil layer was replaced in medium dense conditions in order to meet the criteria for dynamically compactible soil as suggested by FHWA-SA-95–037. By examining the drilled boreholes within the examined area, which was quite uniform, it was possible to assess the impact of the spatial distribution of subsurface soil in the region. Table 1 contains a summary of the technical characteristics of both layers.

Geofoam

The geofoam used was ionolite with a density of 6.6 kg/m^3 and compressive strength of 23 kPa. This product is commonly used in the building construction.

Testing procedure

Using a cylindrical steel tamper that had a diameter of 0.75 m, a height of 0.75 m, and a weight of 1.65 tons, dynamic excitation consisting of a non-harmonic short-time vertical force was applied. With a drop height of 3.6 m, 0.06 kJ (6 t.m) of energy was applied. A process scheme is shown in Fig. 2.

Before the barrier was excavated out, the vertical peak particle velocity (PPV) caused by the impact load was recorded at each selected location on an intact field. Then, in accordance with the testing protocol (Table 2), the specified physical conditions were implemented. To do so, a drilling machine was used to dig the barrier holes and trenches as shown in Fig. 3. For two of the tests, geofoam material was installed in the open trenches. In each test, the excitation due to dynamic compaction was applied and the vertical PPVs were recorded at the specified locations.

Table 1 Technical parameters of sub-soils

Geotechnical parameters		Range of depth (m)	Strength classification	Natural moisture (%)	Dry density (kN/m^3)	Cohesion (kPa)	Friction angle (°)	Elastic modulus (kPa)	Poisson's ratio	Shear modulus (kPa)
Layer no	Layer type									
1	SC	0–2	medium dense	12	15	25	31	12,000	0.35	4400
2	CL	> 2	very stiff	15	18	110	7	30,000	0.40	10,700

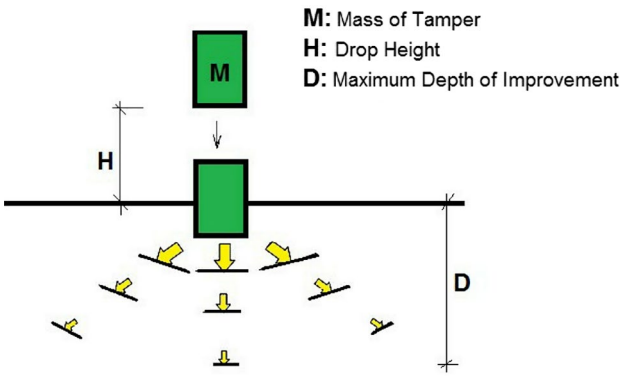

Fig. 2 Schematic pattern of applied transient load in dynamic compaction

Instrumentations

Figure 4 shows the instrumentations' locations and experimental configurations. Figure 5 show images of the testing field and instrumentations. The vertical PPVs were measured using geophones with a natural frequency of 4.5 ± 0.5 Hz. The geophones were deployed in a 1.5×1.5 m gridded triangular area as shown in Fig. 4. The geophones were connected to a 24-channel data logger. In all tests, the data was recorded over the course of 16 s at a frequency of 1 kHz.

The maximum PPVs were essential to this investigation, hence this value could only be ascertained from the geophones' temporal histories. Except for the trenches filled with geofoam, which were tested exclusively at R = 6 m, impact distances (R: distance between the impact site and the barrier) of 3 m and 6 m were evaluated. In each of the performed tests mentioned in Table 2, ten drops were carried out to trace the changes in terms of the densification of the bed. At the end of the tests, owing to the fact that the ground conditions changed with number of impacts, the average PPV was herein considered and reported.

Dimensional analysis was required for better assessment and interpretation of acquired results [45, 46]. Consequently, Eq. (1) is presented to define the contributory factors in the PPV appeared in terms of the impact load.

$$\mathrm{PPV} = \mathrm{f}(Di,\ Tb,\ Lb,\ \mathrm{d},\ Vss,\ Vsb,\ \rho s,\ \rho b,\ \xi s,\ \xi b,\ \nu s,\ \nu b) \quad (1)$$

Table 2 Geometric parameters of the tests

Void holes (including 5 adjacent holes)				
Test no.	Test variables			Test conditions
	Hole diameter (m)	Hole depth (m)	Centre-to-centre distance between holes (m)	
1	0.40	2.0	0.4	Constant diameter and depth of holes, but variable centre-to-centre distance bet. holes
2	0.40	2.0	0.9	
3	0.40	1.0	0.9	Constant diameter and centre-to-centre distance bet. holes, but variable depths
4	0.40	1.5	0.9	
2	0.40	2.0	0.9	
5	0.40	2.5	0.9	
2	0.40	2.0	0.9	Constant depth and centre-to-centre distance bet. holes, but variable diameter of holes
6	0.65	2.0	0.9	
Trench barriers				
Test no.	Test Variables			Test conditions
	Trench width (m)	Trench depth (m)	Trench length (m)	
2	0.40	2.00	2.0	Open Trench: constant trench depth, but variable trench plan area (TL)
7	0.65	2.00	4.0	
8	0.65	1.50	4.0	Open Trench: constant trench length and width, but variable depth
7	0.65	2.00	4.0	
9	0.65	2.50	4.0	
10	0.40	2.00	4.0	Trench in-Filled with Geofoam: constant trench depth and length, but variable width
11	0.65	2.00	4.0	

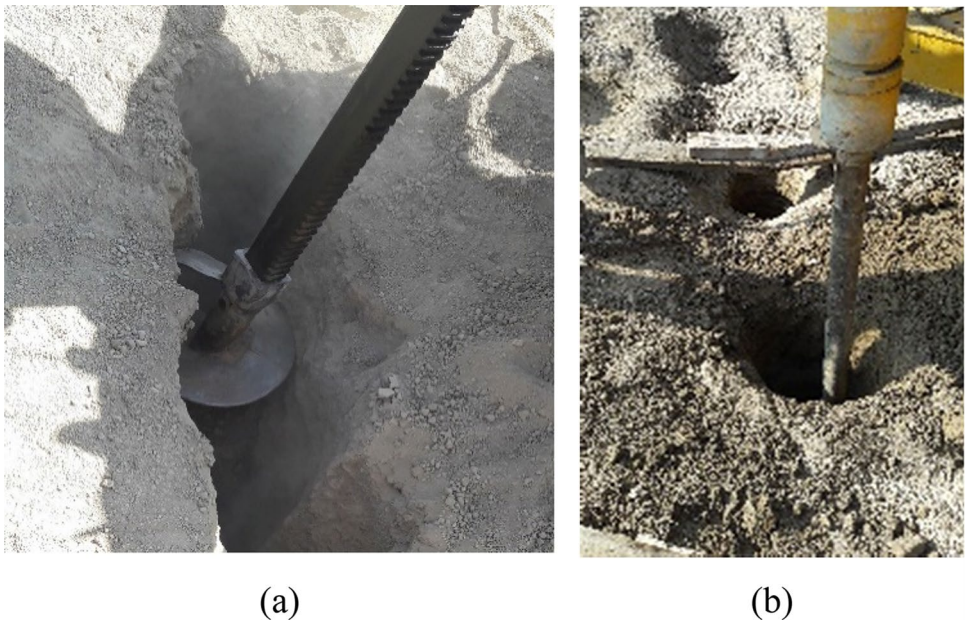

Fig. 3 Images of: **a** open trench barrier; **b** empty hole barrier

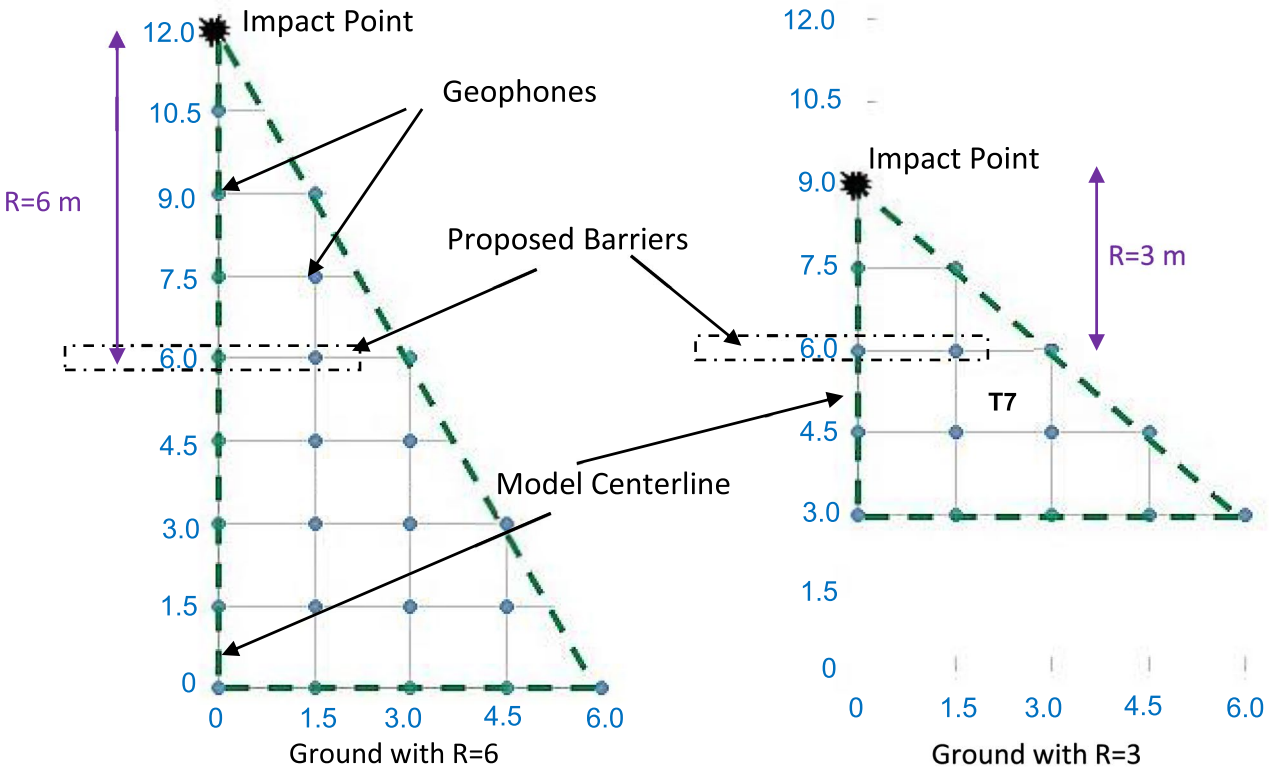

Fig. 4 Instrumentation and experimental configurations

where D_i is the depth of the effect of dynamic compaction based on the Lukas formula [47] and is proportional to the energy applied to the ground ($D_i = n\sqrt{W \cdot H}$ in which W is the tamper mass, H is the falling height and n is usually equal to 0.5), T_b, H_b, and L_b are the thickness, height, and length of the barrier, respectively; d is the distance of the particle from the barrier; V_{ss} and V_{sb} are the shear wave velocity in the soil and the barrier, respectively; ρ_s and ρ_b

Fig. 5 Images of: **a** installation of geophones in ground; **b** falling dynamic compaction tamper

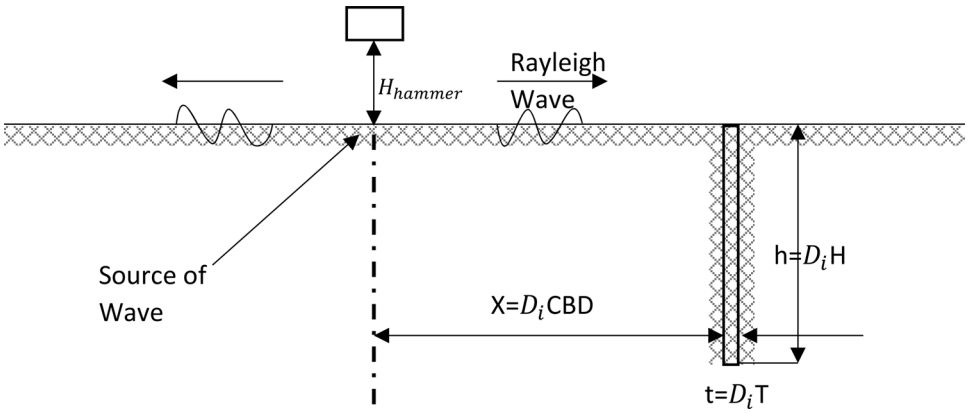

Fig. 6 Schematic of typical vibration isolation system

are the density of the soil and the barrier, respectively; ξ_s and ξ_b are the damping ratio of the soil and the barrier, respectively; and finally, ν_s and ν_b are the Poisson's ratio of the soil, and the barrier, respectively. With the use of dimensional analysis, Eq. (2) consisting of the basic dimensionless contributory factors can be considered.

$$\mathrm{PPV}_{(\text{with Barrier})}/\mathrm{PPV}_{(\text{without Barrier})} = \mathrm{f}\left[T_b/D_i,\ H_b/D_i,\ L_b/D_i,\ d/D_i,\ V_{sb}/V_{ss},\ \rho_b/\rho_s,\ \xi_b,\ \xi_s,\ \nu_b,\ \nu_s\right] \quad (2)$$

Parameters T_b/D_i, H_b/D_i, L_b/D_i, d/D_i were studied, some of which were recognized as effective parameters in previous studies (Ahmad and Al-Hussaini [28, 34], Alzawi [21]). Parameters V_{sb}/V_{ss}, ρ_b/ρ_s, ξ_b/ξ_s, ν_b/ν_s are the ratios of the physical parameters of the barrier to the soil. Assuming the use of similar materials in prototype model, these parameters were disregarded in this study. Previous studies on the subject came to the conclusion that the influence of the soil barrier's Poisson's ratio is negligible and may be disregarded for the usual range of soil Poisson's ratio (0.25 to 0.48). Figure 6 shows a schematic of a typical vibration isolation system, and Table 3 presents the dimensionless parameters of the test. For scaling during the dynamic compaction tests, all parameters having dimension L were normalized to$D_i = \left(0.57 \times \sqrt{6}\right)m$.

Experimental results and discussion

A discussion on how the barrier's dimensionless shape affects its screening effect should come after a source of disturbance has been described. The term "screening effect" describes the act of minimizing or attenuating the adverse effects of waves on buildings by applying shielding or protective measures like wave barriers.

General properties of ground response

To assess the effects of barrier geometry on the screening effect, all dynamic compaction tests were conducted under the same initial ground conditions and compaction energy (similar tamper mass and drop height). Figure 7 shows a typical Fourier amplitude spectrum obtained from the recorded signals measured on the ground, in test No.9.

From the PPVs of one sensor to the next, the amount of time was calculated. The interval between two successive

Table 3 Dimensionless test parameters

Parameter	Values	Normalized values
Trench width (thickness)	t = 0.4, 0.65 m	T = 0.29, 0.47
Trench or hole depth	h = 1.0, 1.5, 2.0, 2.5 m	H = 0.72, 1.07, 1.43, 1.79
Trench length	l = 2, 4 m	L = 1.43, 2.86
Trench plan area	tl = 0.8, 2.6 m^2	TL = 0.41, 1.33
Hole diameter	di = 0.40, 0.65 m	Di = 0.29, 0.47
Centre-to-centre distance between holes	ccdh = 0.4, 0.9 m	CCDH = 0.29, 0.65
Compaction to barrier distance	cbd = 3, 6 m	CBD = 2.15, 4.3

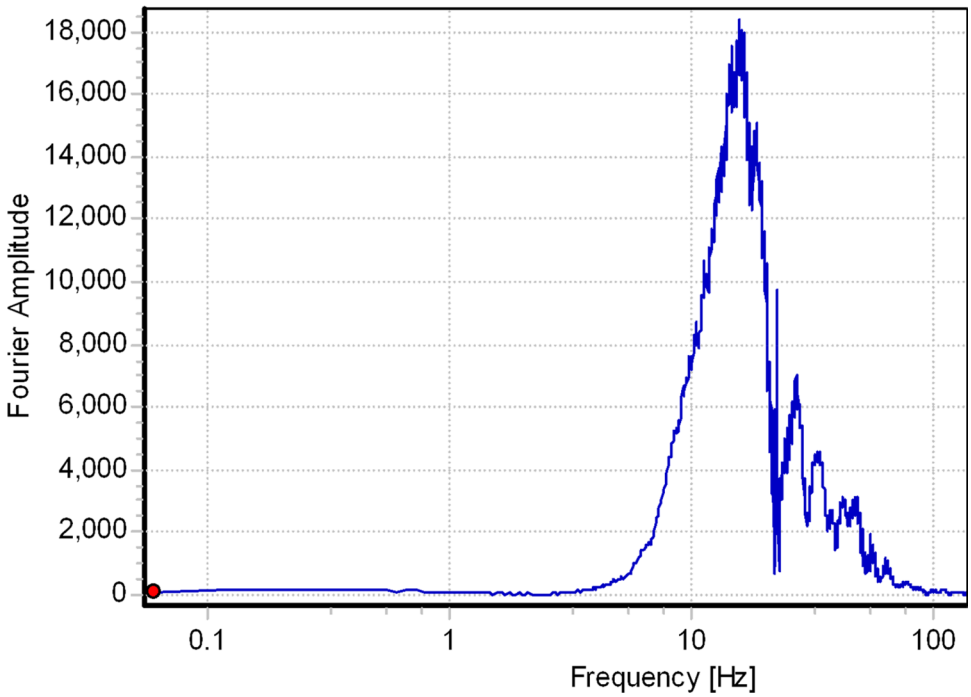

Fig. 7 Typical time-history Fourier amplitude spectrum of signals measured on the ground in test No.9

placed sensors was not equal because the impact wave and damping were non-harmonic. For multiple experiments, the average time delay between geophones was roughly 6 ms. Therefore, considering the geophones distance of 1.5 m, the average velocity of Rayleigh wave propagation is obtained as 250 m/s. An average time period (T) and, in turn, frequency of the wave (*f*) were obtained 40 ms and 25 Hz, respectively. Moreover, the average wave length of impulses was estimated to be about 10 m ($\lambda = 250 \times 0.040 = 10$ m).

To evaluate the performance of the proposed physical experimental model and instrumentations, the PPVs measured in ground without a barrier were compared with the results obtained by Mayne et al. [48] and Lukas [47]. As it can be seen in Figs. 8 and 9, the measurements fall into the range as previous researchers highlighted.

Velocity reduction factor (VRF)

The soil particle velocity at a particular site is often used in practice to analyse the impact of transmitted vibration. The effectiveness of a protective system may be defined in terms of a decrease in the soil particle velocity as the peak velocities have been chosen as a representation of ground vibration. Thus, the results were presented in the form of vertical PPV reduction factor (VRF). This can be defined as the ratio of a PPV (in vertical direction) with barriers $(PPV)_{Barr}$ to that of intact ground $(PPV)_{Intact}$.

Reliability of measured velocities

The intensity of the applied energy was determined by looking at the data the geophones recorded after the test, and it was discovered that some of the geophones had achieved their maximum capacity (velocity of 8 mm/s). It was determined that the collected results at a distance of more than

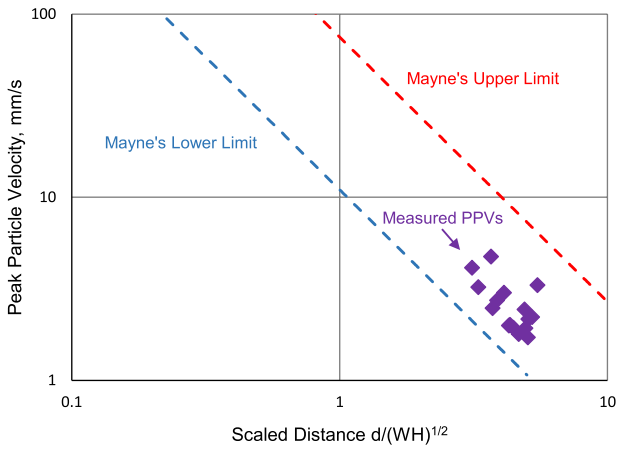

Fig. 8 Influence of normalized barrier dimensions on screening effectiveness of empty trenches at different distances after barrier: **a** effect of normalized trench depth; **b** effect of normalized trench plan area (thickness × length)

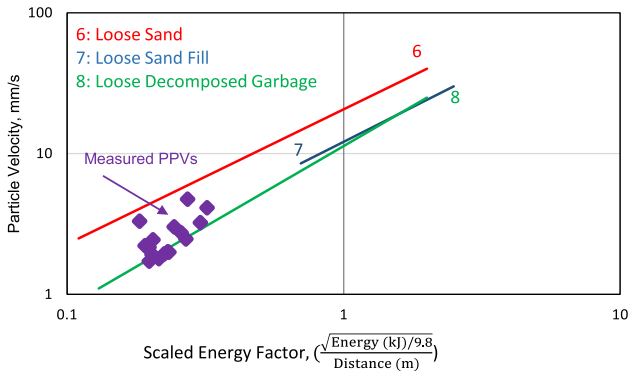

Fig. 9 Influence of normalized barrier dimensions on screening effectiveness of trench in-filled with geofoam (L = 2.86, H = 1.43) at different distances after barrier: **a** effect of normalized trench thickness; **b** effect of trench filler (air or geofoam)

6 m from the impact location were trustworthy. Therefore, for tests performed in smaller ground in which the distance from the impact point to the barrier was 3 m (CBD = 2.15), only a few of measured velocities after the barrier location could be considered reliable.

Given the above, only reliable data are presented and discussed in this paper.

Effect of trench barriers

Figure 10 shows the influence of the empty trench depth on reducing the induced vibrations in comparison with the intact ground. Figure 10a shows that, as barrier depth increased, the screening effect improved, especially at a closer distance behind the empty trench. Consequently, the trench with a normalized depth of $H = 1.79$ had the best screening effect of reducing PPV. Figure 10b shows the trench plan area (width × length) effect. As the trench plan area increased, the screening effect increased, especially at a closer distance after the empty trench (at a normalized distance of 1.25). D (normalized distance) is relation of distance to $D = (0.57 \times \sqrt{6})$ m.

Figure 11 shows the effect of barrier dimensions on reducing the PPV of a trench in-filled with geofoam at different distances behind the barrier. Figure 11a shows the effect of trench width and Fig. 11b shows the effect of the trench filler (air and geofoam). These numbers show an increase in the screening effect of thicker geofoam-filled trenches of roughly 20%. Particularly at a closer distance following the empty trench (to a normalized distance of 1.25), there was a stronger screening effect (at least 5%) for the empty trenches compared to the geofoam-filled ones.

Diffraction effects on amplification of wave velocity behind the barrier

In Figs. 8 and 9, it can be seen that VRF was more or less close to a value of 1 adjacent to the barrier. This reached a minimum value at a normalized distance of 1.25. Beyond this point, the VRF value rises and eventually reaches values larger than 1 as the distance grows. Wave diffraction may be responsible for these two actions. Wave superposition may result from the frequent wave diffraction from a barrier's bottom and side edges. The combinations of in-phase waves in diffraction can increase the wave velocity before or after a barrier. It should be emphasized that a similar intensification effect was noticed in other studies, such as those on classic trenches or meta-barriers in selected areas [5, 49–60].

Existence of two layered soil causes noticeable Rayleigh waves during dynamic compaction in terms of the reflection of SV waves from the boundary among layers towards the ground surface. The induced Rayleigh wave moves near the ground surface and carries nearly two-thirds of the vibration energy [61]; so, it has the major effects on measured vertical PPV on the ground surface. Therefore, diffraction of Rayleigh waves from side and bottom edges of barriers in two layered soil would play a major role in increase of vertical PPV values measured behind barrier.

Figure 12 shows the different zones in terms of wave propagation, and interfering mechanisms. The zones were defined by measurements and VRF values as zone A (or A'), zone B (or B'), and zone C (or C'). In zones A (or A') and C (or C'), the governing waves were normally refracted waves which produced VRF values of less than 1. In turn, the diffracted waves that passed by the bottom edge and side edges of barrier interfered with the normally refracted waves and formed zones B and B', respectively. Diffraction makes the wave aftereffects tensified which normally occur after refraction and resulted in values of less than 1 in the

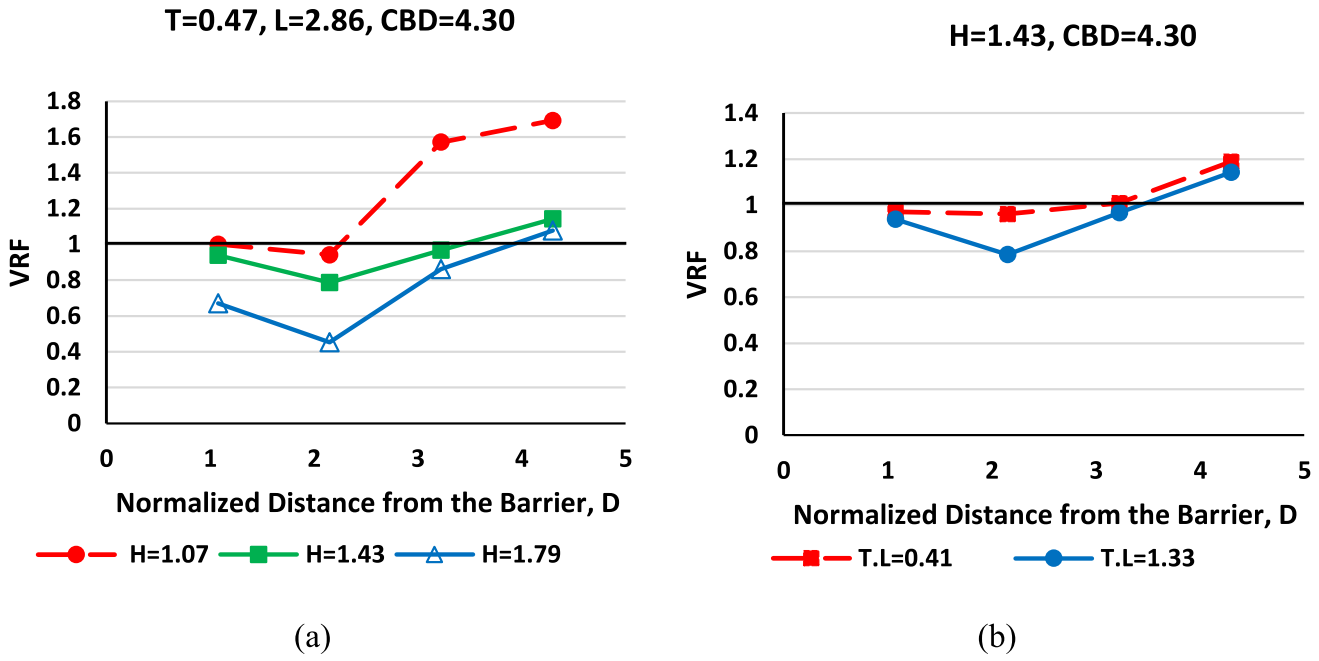

Fig. 10 Measured PPVs vs. those obtained by Lukas [47]

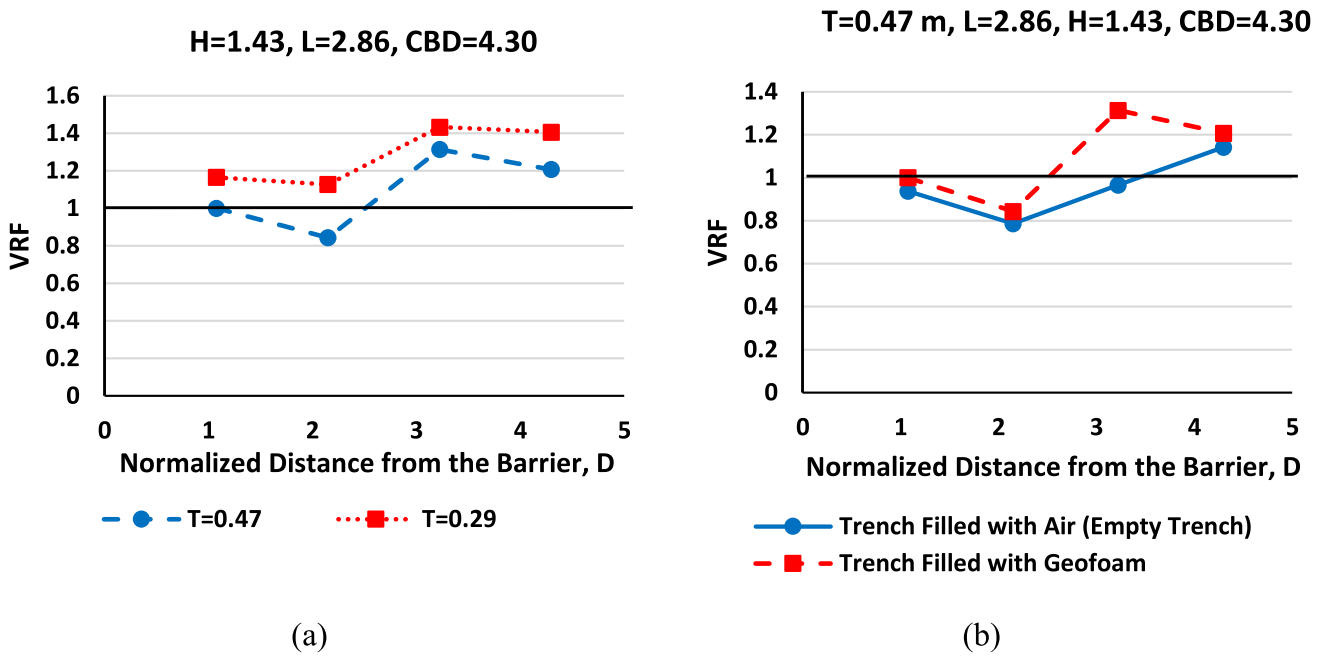

Fig. 11 Influence of normalized barrier dimensions on screening effectiveness of trench in-filled with geofoam (L = 2.86, H =1.43) at different distances after barrier: a effect of normalized trench thickness; b effect of trench filler (air or geofoam)

VRF diagram versus the distance from the barrier in zones A and C (or A' and C') and of more than 1 in zones B or B'. The screening effect generated VRF values larger than 1 in these zones because the impact of diffraction was stronger than the velocity reduction effect of the barrier. The highest barrier reduction impact in Figs. 9 and 11 provided the smallest VRF value after the barrier by offsetting the diffraction effect at the normalized distance of 1.25.

As an example, the mentioned diffraction effects on amplification of waves after a trench barrier with normalized dimensions of T = 0.29, H = 1.43, L = 2.86 are indicated in Fig. 13 and Fig. 14 by numerical modelling using Plaxis.3D

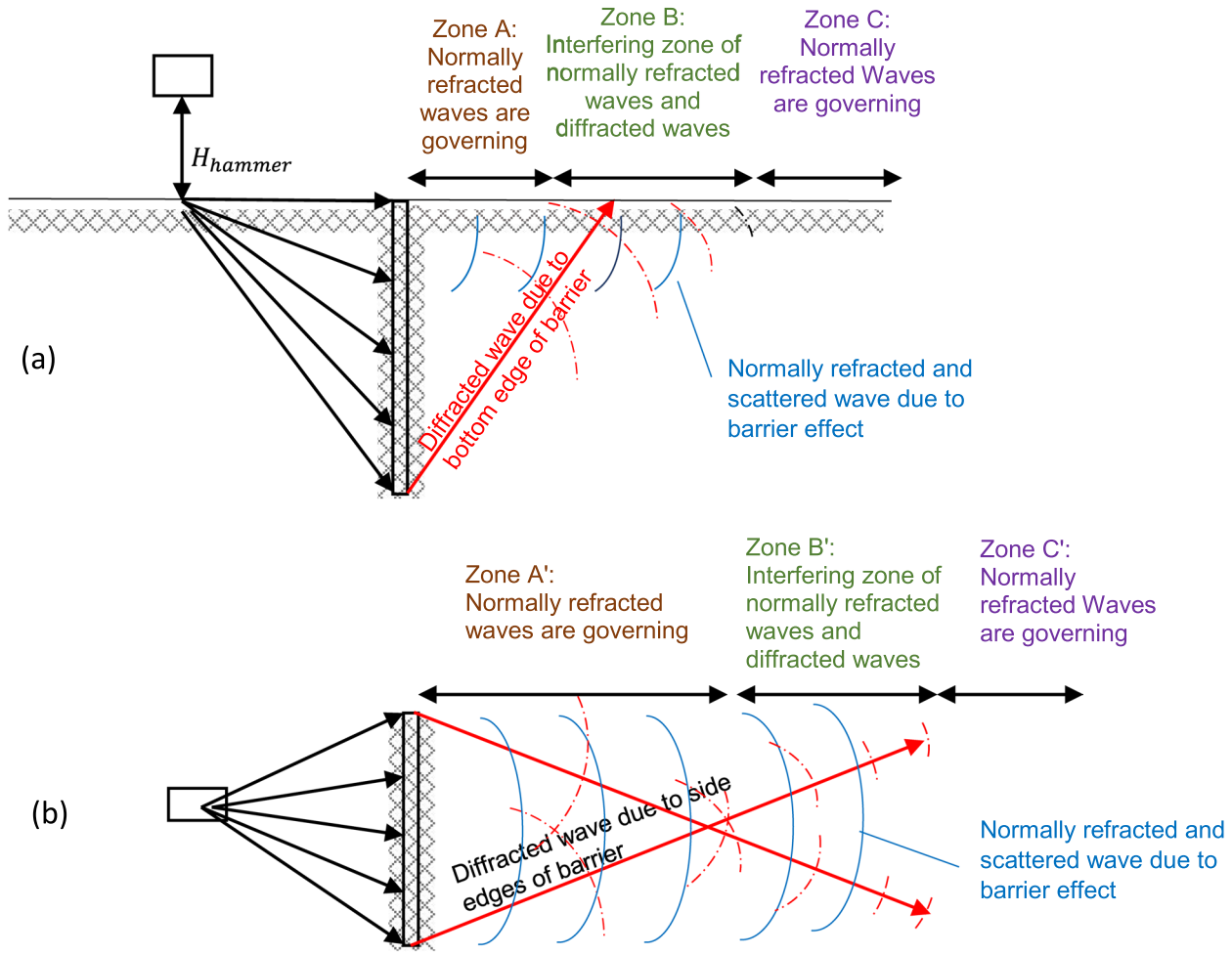

Fig. 12 Schematic of vibration isolation system: **a** section view of wave diffracted by bottom edge of barrier; **b** plan view of wave diffracted by side edges of barrier

software. The parameters and assumptions of this modelling will be briefly discussed in "Experimental results and discussion" section and "Introduction" section, despite the fact that it is not the major subject or emphasis of this article and was only done in this part to better illustrate the phenomena of diffraction. Figure 13 shows diffraction effect on the amplification of ground vibrations by comparing the contours of vertical velocity when hammer impact applied to the ground at different elapsed times of 10, 20, 30 and 40 ms.[1] It is evident in Fig. 13c and Fig. 13d that amplification of velocity occurs before and after the barrier as Rayleigh wave reaches the barrier.

Diffraction effects on amplification can be observed in Fig. 14 by the comparison of vertical velocity contours on ground surface with and without trench barriers at an elapsed time of 40 ms.

The amount of diffraction (sharpness of wave bending) increased with a decrease in size of obstacle through which the wave passed. Therefore, if a barrier is sufficiently large, it is likely that unfavourable diffraction effects will be reduced, resulting in less interference and producing a lower VRF value.

Numerical modelling

The area of interest must be sufficiently far from the reflecting border since the transmitted and reflected waves from the model's boundary have a significant impact on it. Therefore, the model's chosen dimensions are (25, 25, 25 m). The soil is modelled as a two layered homogeneous and isotropic half space. To apply a special boundary condition, viscous boundaries are applied to the bottom and at X max and Y max direction for 3D model.

Based on data analysis from field test geophones, the vibration source is modelled as a single pulse of a vertical

[1] 40 ms is the time period of impact.

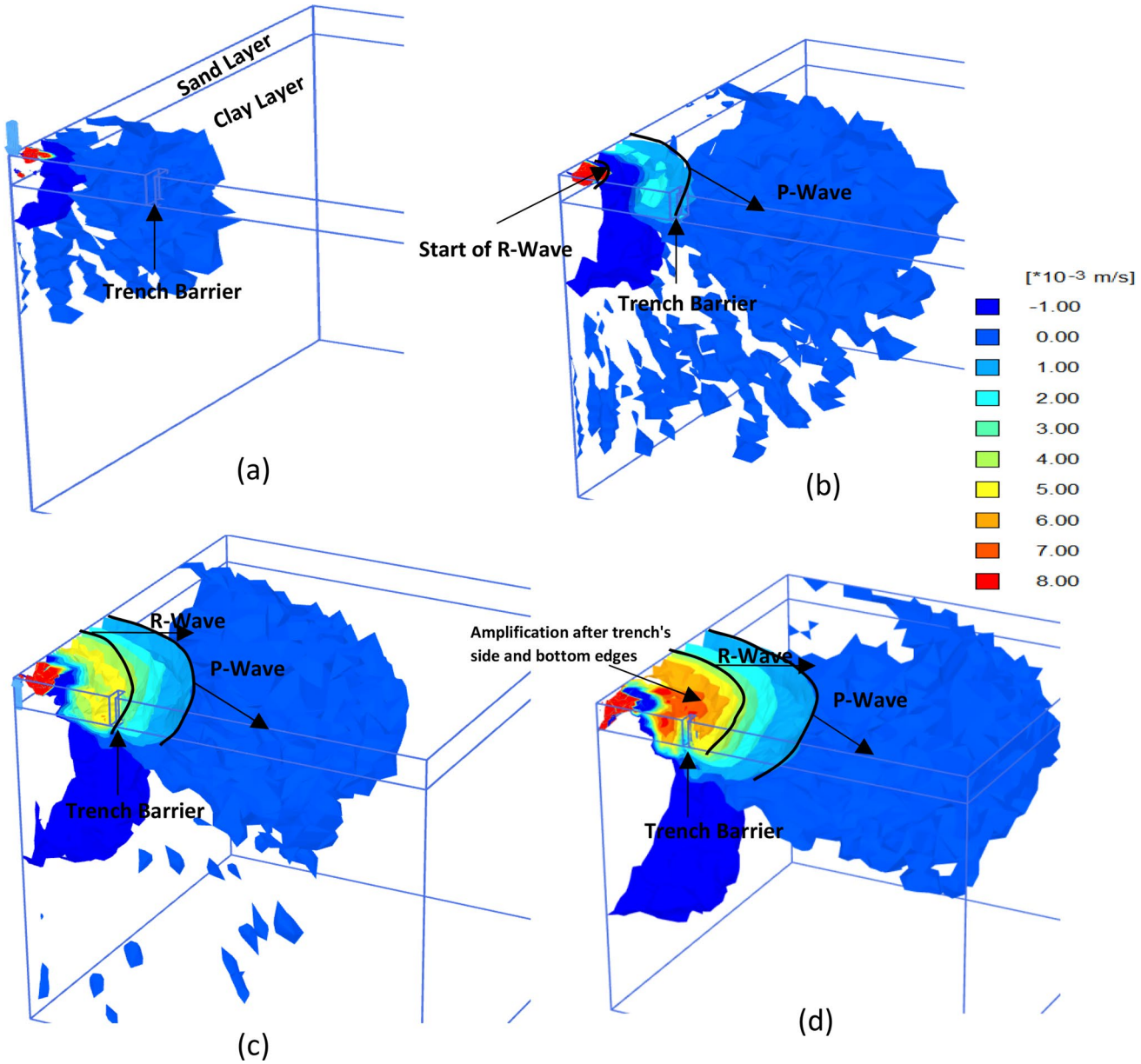

Fig. 13 Diffraction effects on amplification of velocity for the ground with trench barrier ($H = 2$ m, $t = 0.4$ m, $L = 4$ m) by comparing the vertical velocity contours when hammer impact applied at different elapsed times of **a** 10 ms; **b** 20 ms; **c** 30 ms; **d** 40 ms

harmonic load with an amplitude of 3201, a frequency of 25 Hz, and a dynamic time interval of 0.04 s.The soil properties for following analysis are considered the same as those measured in the field test, which are presented in Table 1. Besides, material model of sand layer and clay layer are considered HS-small and Mohr–Coulomb, respectively and their Rayleigh damping coefficients are considered as ($\alpha = 3.888$, $\beta = 0.00000926$) and ($\alpha = 0.9220$ and $\beta = 0.0001562$), respectively.

The field test results for the ground without a barrier and the ground with a trench barrier (H = 1.43, T = 0.29, L = 2.86) were used to verify the created model. Figure 15 shows the experimental and analytical peak particle velocities. As indicated in these figures, the Plaxis 3D model results are in line with the trends in the experimental results, and there is a reasonable agreement between the vertical soil particle velocities, obtained.

Also, the Nash–Sutcliffe model efficiency coefficient (NSE), which is a normalized statistical parameter that determines the relative magnitude of the residual variance (noise) compared to the measured data variance (information), is calculated as 0.83 and 0.98 for presented data in Fig. 15a, b, respectively. The NSE can be computed based on Eq. (3):

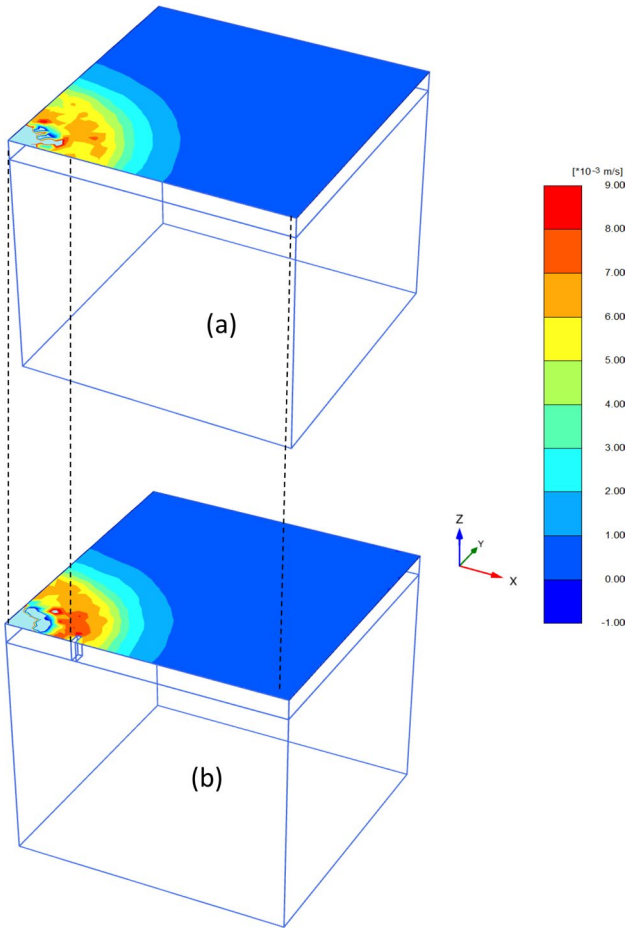

Fig. 14 Diffraction effects on amplification of velocity by comparing the vertical velocity counters on the surface of **a** Natural ground without barrier and **b** Ground with trench barrier

$$NSE = 1 - \frac{\sum_{i=1}^{n} \left(Y_i^{obs} - Y_i^{sim}\right)^2}{\sum_{i=1}^{n} \left(Y_i^{obs} - Y^{mean}\right)^2} \quad (3)$$

where Y_i^{obs} is the ith observation for the constituent being evaluated, and Y_i^{sim} is the ith simulated value for the same constituent. Ymean is the mean of the observed data, and n is the total number of observations. The NSE ranges between $-\infty$ and 1.0, with NSE = 1 being the optimal value. The values between 0.0 and 1.0 are generally viewed as acceptable levels of performance. However, NSE < 0.0 below 0.0 indicate that the mean observed data is a better predictor than the simulated value, which indicates unacceptable performance of a model.

Given the above, the calculated NSE values indicates a good model results, as well.

Effect of hole barriers

Figure 16 and Fig. 17 show the influence of the barrier dimensions on screening effects of void holes at different distances after the barrier. Figure 17 shows that, as the barrier depth increased, the VRF values decreased. Consequently, the holes with a normalized depth of $H = 1.79$ produced the lowest VRF values. Figure 17a shows the effect of the centre-to-centre distance between the holes. As can be observed, the VRF values grew as the center-to-center distance did as well. This has to do with the fact that more waves remain on their regular route and speed without deviating in the area between holes when they hit holes that are further apart. Figure 17b shows that, as the diameter of the holes increased, the VRF values decreased.

Diffracted waves were generated in the spaces among the void holes, as well as past the bottom and side edges of the barrier. It was found that diffraction primarily was the governing phenomenon in the tested void holes. The test results indicated that 1st to 3rd geophones after barrier were located in zone B of Fig. 12 and, with an increase in the normalized distance for 4th geophone, the VRF diagrams entered zone C. The maximum VRF value was reached at a normalized distance of 1.75 and was related to the strongest diffraction at this distance.

As shown in "Reliability of measured velocities" section, not all of the velocities observed after the barrier were accurate on ground with a compaction-to-barrier distance of 3 m (CBD = 2.15). This made it impossible to thoroughly compare the various barriers using the test data. Table 4 does identify the instances when trustworthy data was provided. At CBD = 2.15, screening effect varied from the best condition (VRF = 0.4) which was related to the empty trench ($T = 0.47$, $L = 2.86$, $H = 1.79$) to the worst condition (VRF = 1.13) which was related to the empty holes. General comparison of the VRF values for the barriers in this section (CBD = 2.15) with those of previous sections (CBD = 4.30) in Table 5; indicated that, as the source of compaction became closer to the barrier, the screening effect increased at the same normalized distance recorded after the barrier. From a comparison of reducing trend of data in Table 5 for the empty trench barrier ($T = 0.47$, $L = 2.86$), it can be concluded that, to achieve a specific VRF value at a specific distance after the barrier, larger dimensions are required for more distant sources of compaction. For example, at a normalized distance of 4.44, larger barrier dimensions (especially for depth) could be required for more distant sources of compaction (CBD = 4.30 at $H > 1.79$ and at CBD = 2.15 at $H = 1.07$) to obtain a VRF of about 0.8.

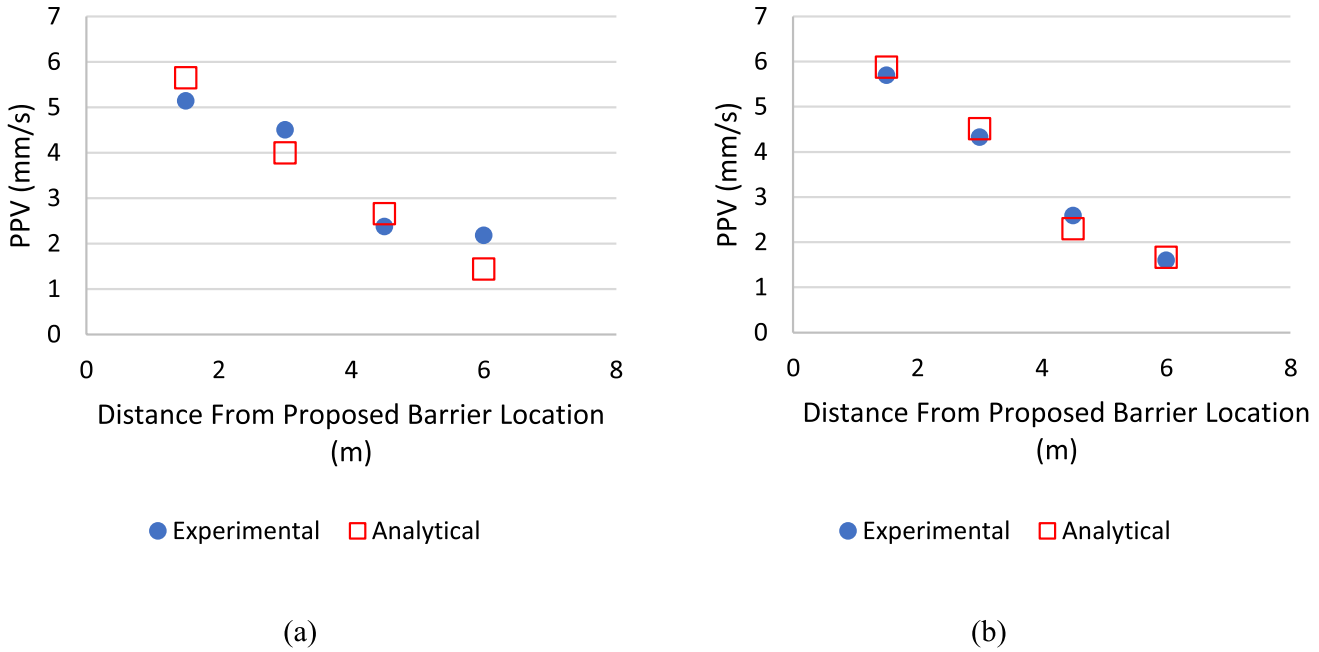

Fig. 15 Validation of numerical modelling based on the result of field test: **a** ground without barrier; **b** ground with empty trench barrier of (H = 1.43, T = 0.29, L = 2.86)

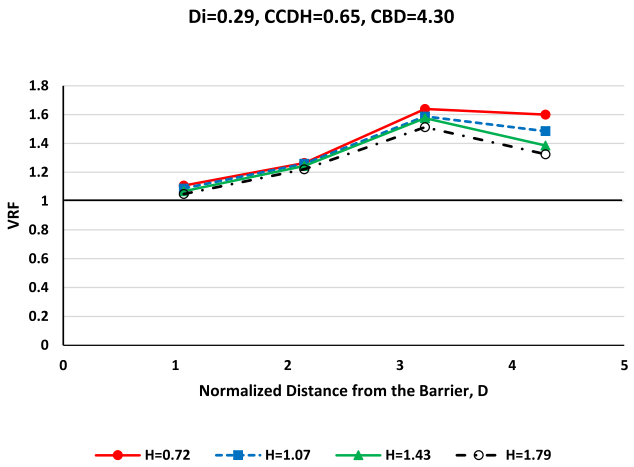

Fig. 16 Influence of normalized dimensions of barrier on screening of void holes at normalized depth

Applicability of the results

The ground-borne vibrations produced due to, for instance, dynamic compaction can exert unfavourable effects on neighbouring structures. Some studies and standards presented guidelines to restrict the PPV of nearby structures based on the type of structure and the characteristics of the transferred waves. According on the impact's duration (short-term vs. long-term vibrations), DIN 4150.3 categorizes the side effects of impact vibrations on neighbouring buildings. The frequency and duration of short-term vibrations are not adequate for causing appreciable increases in vibration from resonance in a given structure, and they do not build over time enough to produce material fatigue. Long-term vibration is any vibration that does not fall into the definition of short-term vibration. Using this classification, dynamic compaction can be classified as a short-term vibration. Table 6 shows the guideline values for the vibration velocity, $v_{i,max}$, used to evaluate the effects of short-term vibration on structures.

Table 6 shows that, for a residential structure and waves having a frequency range of < 10 Hz, the PPVs induced by dynamic compaction should be limited to 5 mm/s. This means that, by estimating the scaled distance from the average line of Mayne's graph in Fig. 18 (between maximum and minimum range), structures with distances of less than about 3.1 times the square root of dynamic compaction energy ($\sqrt{W \cdot H}$) from source of compaction could be at risk of unfavourable effects. In this situation, wave barriers can effectively reduce the PPVs to acceptable values for structures near dynamic compaction sources.

The findings of this study may be seen as a first step in identifying the practical criteria that will be utilized in designing barriers against unfavourable wave effects based on the information currently available in the area of decreasing ground vibrations caused by dynamic compaction. As a practical example, let to consider a structure located in a distance of about $2.9 \cdot \sqrt{W \cdot H}$ from a dynamic compaction source which could, on average, lead to an unacceptable

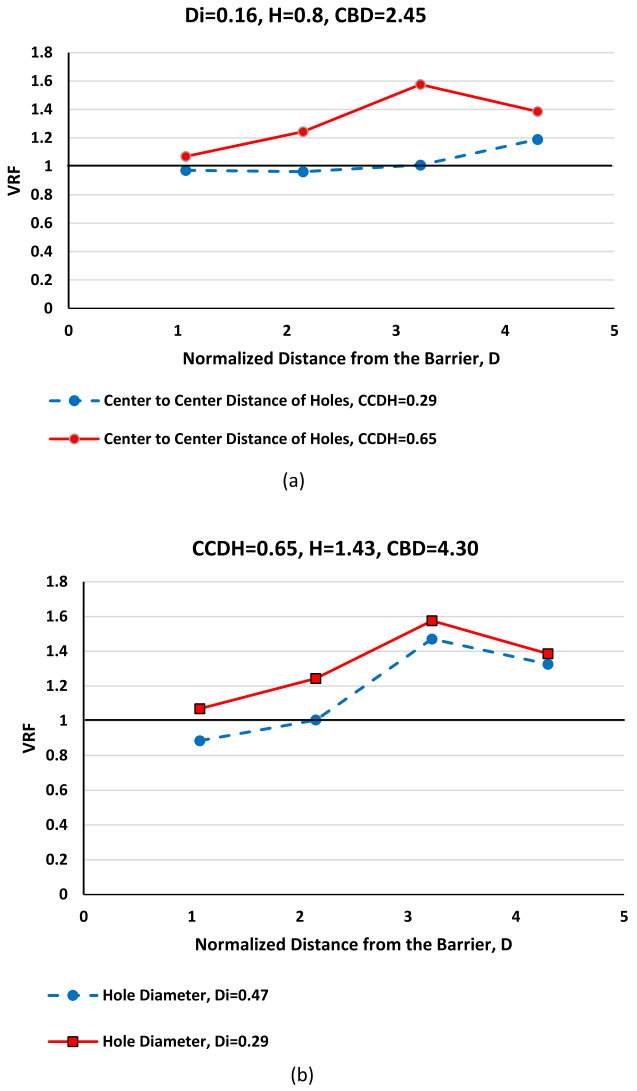

Fig. 17 Influence of normalized dimensions of barrier on screening of void holes by distance from barrier: **a** normalized centre-to centre distance; **b** normalized diameter

PPV of about 6 mm/s. Using an empty trench with normalized dimensions ($T=0.47$, $L=2.86$, $H=1.79$) at a distance of about $1.9 \cdot \sqrt{W \cdot H}$[2] from the source (about $1 \cdot \sqrt{W \cdot H}$[3] from proposed structure) will reduce the induced PPV to an acceptable value of at least 3 mm/s ($=0.5 \times 6$ mm/s). However, in case of using five void holes (CCDH = 0.65, $H=1.43$, $D_i=0.47$) at a distance of about $2.4 \cdot \sqrt{W \cdot H}$ from the source (about $0.5 \cdot \sqrt{W \cdot H}$ from proposed structure) the induced PPV get reduced to a relatively acceptable value of about 5.1 mm/s ($=0.85 \times 6$ mm/s). To show a better description for application of the obtained result, the relevant safe distance of empty trench barrier with normalized dimensions of T = 0.47, L = 2.86, H = 1.79 and 5-void-hole barrier with normalized dimensions of CCDH = 0.65, H = 1.43, Di = 0.47 from residential buildings are suggested in Table 7 for the specific guidelines' values.

Conclusions

An experimental testing program was carried out to study the protective effectiveness of open trenches, open holes and trenches filled with geofoam as wave barriers in the attenuation of induced vibrations in the aftermath of dynamic compaction. The dynamic compaction vibration was simulated using a tamper drop. The protective effectiveness of the wave barriers with different dimensions and location to the impact load was evaluated based on the reduction of the soil particle velocity. The following conclusions were drawn based on analysis of the results:

- The field results showed that empty trench barrier can be considered a practical alternative for wave scattering with a protective effectiveness of 50%.
- All barriers were found to be generally more effective at $H \geq 1.79$ (optimum barrier normalized depth).
- Trench barriers with a normalized thickness (T) of over 0.47 and a normalized plan area (TL) of over 1.33 provided relatively good isolation effects.
- The void holes with normalized hole diameters (D_i) of over 0.47 and normalized centre-to-centre distances between holes (CCDH) of less than about 0.29 provided relatively good isolation effects shifting VRF numbers to values less than 1.
- The results showad that larger barrier dimensions (especially for depth) were required as CBD ratio (normalized compaction to barrier distance) increased to achieve the same level of improvement in the system effectiveness.

It should be noted that the current conclusions only apply to the implemented variations, which include the applied dynamic compaction energy (6 t.m), the dimensions of the barriers, the distance of the barriers from the impact source, and the ground properties. Also based on the difficulties of field tests and PPV measurements and considering the main purpose of the study which was a comparative study on the effects of different factors of considered wave barriers on ground vibration, the results of the current study have not been evaluated for reproducibility. Consequently, further research is needed to fulfil this technical matter. Additionally, the cost–benefit analysis can be carried out in the future studies.

[2] 40 ms is the time period of impact

[3] Normalized distance from the barrier, D=0.87

Table 4 Test results for compaction-to-barrier distance of 3 m (CBD = 2.15)

Type of barrier	Barrier conditions	Influence of barrier versus velocity reduction factor					
Empty trench	$H = 1.43$, $TL = 1.33$	Normalized distance from centre of barrier, D	3.23	3.56	3.72	4.44	5.26
		VRF	0.99	0.99	1.00	0.70	0.74
Empty trench	$T = 0.47$, $L = 2.86$ ($H = 1.07$ to 1.79)	Normalized distance from centre of barrier, D	4.44			5.26	
	$H = 1.07$	VRF	0.77			0.91	
	$H = 1.43$		0.70			0.74	
	$H = 1.79$		0.70			0.74	
Empty holes	$D_i = 0.29$, $H = 1.43$, CCDH = 0.29	Normalized distance from centre of barrier, D	3.23			3.72	
		VRF	0.89			1.00	
Empty holes	$D_i = 0.47$,	Normalized distance from centre of barrier, D	4.44			5.26	
	$H = 1.43$,						
	CCDH = 0.65	VRF	1.13			0.99	
Empty holes	$D_i = 0.29$,	Normalized distance from centre of barrier, D	4.44			5.26	
	$H = 1.79$						
	CCDH = 0.65	VRF	0.82			1.13	

Table 5 VRF values barrier conditions at CBD = 2.15 and CBD = 4.30

Type of barrier	Barrier conditions	Influence of barrier VRF			
Empty trench	$H = 1.43$, $TL = 1.33$	Normalized distance from centre of barrier, D		3.23	4.44
		VRF	CBD = 2.15	0.99	0.70
			CBD = 4.30	0.97	1.15
Empty trench	$T = 0.47$, $L = 2.86$ ($H = 1.07$ to 1.79)	Normalized distance from centre of barrier, D		4.44	
	$H = 1.07$	VRF	CBD = 2.15	0.77	
			CBD = 4.30	1.69	
	$H = 1.43$		CBD = 2.15	0.70	
			CBD = 4.30	1.14	
	$H = 1.79$		CBD = 2.15	0.70	
			CBD = 4.30	1.08	
Empty void holes	$D_i = 0.29$, $H = 1.43$, CCDH = 0.29	Normalized distance from centre of barrier, D		3.23	3.72
		VRF	CBD = 2.15	0.89	1.00
			CBD = 4.30	1.00	1.05
Empty void holes	$D_i = 0.47$, $H = 1.43$, CCDH = 0.65	Normalized distance from centre of barrier, D		4.44	
		VRF	CBD = 2.15	1.13	
			CBD = 4.30	1.33	
Empty void holes	$D_i = 0.29$, $H = 1.79$ CCDH = 0.65	Normalized distance from centre of barrier, D		4.44	
		VRF	CBD = 2.15	0.82	
			CBD = 4.30	1.33	

Table 6 Guideline values for $v_{i,max}$ for effects of short-term vibration on structures as proposed by DIN 4150.3: 2016–12

Type of structure	Guideline values for $v_{i,max}$ in mm/s				
	Foundation frequency, all directions, $i=x,y,z$			Topmost floor, horizontal direction, $i=x, y$	Floor slabs, vertical direction, $i=z$
	1–10 Hz	10–50 Hz	50–100 Hz	all frequencies	all frequencies
Buildings used for commercial purposes, industrial buildings and buildings of similar design	20	20–40	40–50	40	20
Residential buildings and buildings of similar design and occupancy	5	5–15	15–20	15	20
Structures that because of their particular sensitivity to vibration, cannot be classified in the previous rows, but are of great intrinsic value (e.g. listed buildings)	3	3–8	8–10	8	20

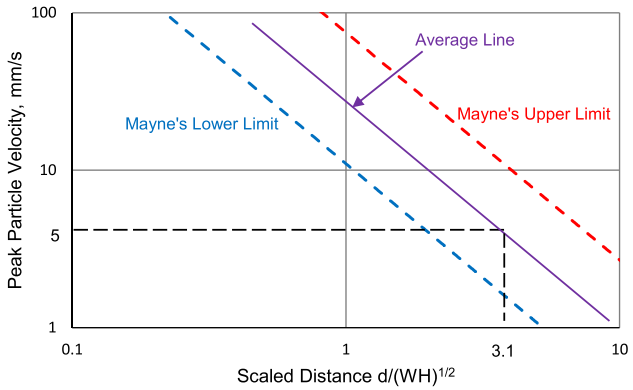

Fig. 18 Obtaining the minimum safe distance from a source of compaction for acceptable PPV of 5 mm/s using the average line between minimum and maximum limits in Mayne et al. [48]

Table 7 Suggestions for safe distance of empty trench barrier (normalized dimensions of $T=0.27$, $L=1.6$, $H=1.0$) and 5-void-hole barrier (CCDH = 0.37, $H=0.8$, $D_i=0.27$) from residential buildings (acceptable PPV values from DIN 4150.3: 2016–12)

Frequency level of PPV	1–10 Hz	10–50 Hz	+50 Hz
Guideline values for PPV (mm/s)	5	5—15	15 – 20
Unsafe normalized distance of building (distance from source/$\sqrt{W \cdot H}$) from source of compaction	< 3.1	< 3.1—< 1.45	< 1.45—< 1.2
Range of unsafe normalized distance of building from source of compaction (distance from source/$\sqrt{W \cdot H}$) for effective use of proposed empty trench barrier	2.0 ~ 3.1	(2.0 ~ 3.1)–(0.95 ~ 1.45)	(0.95 ~ 1.45)–(0.86–1.2)
Normalized distance of proposed empty trench barrier from residential building (barrier distance from building/$\sqrt{W \cdot H}$) for acceptable PPV values induced by dynamic compaction	1.0	1.0–0.9	0.9–0.7
Range of unsafe normalized distance of building from source of compaction (distance from source/$\sqrt{W \cdot H}$) for effective use of proposed void holes barrier	2.85 ~ 3.1	(2.85 ~ 3.1)–(1.3 ~ 1.45)	(1.3 ~ 1.45)–(1.05–1.2)
Normalized distance of proposed void-hole barrier from residential building (barrier distance from building/$\sqrt{W \cdot H}$) for acceptable values of PPV induced by dynamic compaction	0.5	0.5	0.5

Acknowledgements The first author would like to thank Zamiran Consulting Engineers for their equipment support

Funding This study was carried out under no financial resources.

Declarations

Conflict of interest It is confirmed that this paper has not any conflict of interest and it is original.

References

1. Abbaszadeh Shahri A, Khorsand Zak M, Abbaszadeh Shahri H (2022) A modified firefly algorithm applying on multi-objective radial-based function for blasting. Neural Comput Appl 34:2455–2471. https://doi.org/10.1007/s00521-021-06544-z
2. Pak TU, JoHan GRUC (2022) Prediction of characteristic blast-induced vibration frequency during underground excavation by using wavelet transform. Front Struct Civ Eng 16(8):1029–1039. https://doi.org/10.1007/s11709-022-0861-x
3. Xue X, Yang X (2014) Predicting blast-induced ground vibration using general regression neural network. J Vib Control 20(10):1512–1519
4. Erarslan K, Uysal O, Arpaz E, Akif Cebi M (2008) Barrier holes and trench application to reduce blast induced vibration in Seyitomer coal mine. Environ Geol 54:1325–1331. https://doi.org/10.1007/s00254-007-0915-3
5. Woods RD (1968) Screening of surface waves in soil. J Soil Mech Found Eng (ASCE) 94(SM4):951–979. https://doi.org/10.1061/JSFEAQ.0001180
6. Dasgupta B, Beskos DE, Vardoulakis IG (1990) Vibration isolation using open or filled trenches Part 2: 3-D homogeneous soil. Comput Mech 6:129–142. https://doi.org/10.1007/BF00350518
7. Adam M, von Estorf O (2005) Reduction of train-induced building vibrations by using open and filled trenches. Comput Struct 83(1):11–24. https://doi.org/10.1016/j.compstruc.2004.08.010
8. Saikia A, Das UK (2014) Analysis and design of open trench barriers in screening steady-state surface vibrations. Earthq Eng Eng Vib 13:545–554
9. Majumder M, Ghosh P (2016) Intermittent geofoam in-filled trench for vibration screening considering soil nonlinearity. KSCE J Civ Eng 20:2308–2318. https://doi.org/10.1007/s12205-015-0267-6
10. Haupt WA (1981) Model tests on screening of surface waves. In: Proceedings of the tenth international conference on soil mechanics and foundation engineering, vol 3. Stockholm, p 215–22
11. Erkan C, Seyhan F, Gunay B, Ilyas C, Osman K (2009) Field experiments on wave propagation and vibration isolation by using wave barriers. Soil Dyn Earthq Eng 29:824–883. https://doi.org/10.1016/j.soildyn.2008.08.007
12. Comina C, Foti S (2007) Surface wave tests for vibration mitigation studies. J Geotech Geoenviron Eng 133:1320–1324
13. Jayawardana P, Achuhan R, Subashi De Silva GHMJ, Thambiratnam DP (2018) Use of in-filled trenches to screen ground vibration due to impact pile driving: experimental and numerical study. J Heliyon. https://doi.org/10.1016/j.heliyon.2018.e00726
14. Tsai PH, Chang TS (2009) Effects of open trench siding on vibration-screening effectiveness using the two dimensional boundary element method. Soil Dyn Earthq Eng 29:865–873. https://doi.org/10.1016/j.soildyn.2008.09.005
15. Andersen L, Nielsen SRK (2005) Reduction of ground vibration by means of barriers or soil improvement along a railway track. Soil Dyn Earthq Eng 25:701–716. https://doi.org/10.1016/j.soildyn.2005.04.007
16. Coulier P, Cuellar V, Degrande G, Lombaert G (2015) Experimental and numerical evaluation of the effectiveness of a stiff wave barrier in the soil. Soil Dyn Earthq Eng 77:238–253. https://doi.org/10.1016/j.soildyn.2015.04.007
17. Dijckmans A, Ekblad A, Smekal A, Degrande G, Lombaert G (2016) Efficacy of a sheet pile wall as a wave barrier for railway induced ground vibration. Soil Dyn Earthq Eng 84:55–69. https://doi.org/10.1016/j.soildyn.2016.02.001
18. Gao GY, Li ZY, Qiu C, Yue ZQ (2006) Three-dimensional analysis of rows of piles as passive barriers for ground vibration isolation. Soil Dyn Earthq Eng 26:1015–1027. https://doi.org/10.1016/j.soildyn.2006.02.005
19. Ma XF, Cao MY, Gu XQ, Zhang BM, Yang ZH, Guan PF (2020) Vibration-Isolation performance of a pile barrier in an area of soft soil in shanghai. Hindawi Shock Vib. https://doi.org/10.1155/2020/8813476
20. Ulgen D, Toygar O (2015) Screening effectiveness of open and in-filled wave barriers: a full-scale experimental study. Constr Build Mater 86:12–20. https://doi.org/10.1016/j.conbuildmat.2015.03.098
21. Alzawi A, Hesham E, Naggar M (2011) Full scale experimental study on vibration scattering using open and in-filled (GeoFoam) wave barriers. Soil Dyn Earthq Eng 31:306–317. https://doi.org/10.1016/j.soildyn.2010.08.010
22. Davies MCR (1994) Dynamic soil structure interaction resulting from blast loading. In: Leung, Lee, Tan (eds) Centrifuge. Balkema, Rotterdam, pp 319–324
23. Wang JG, Sun W, Anand S (2009) Numerical investigation on active isolation of ground shock by soft porous layers. J Sound Vib 321:492–509. https://doi.org/10.1016/j.jsv.2008.09.047
24. Murillo C, Thorel L, Caicedo B (2009) Ground vibration isolation with GeoFoam barriers: centrifuge modelling. Geotext Geomembr 27:423–434. https://doi.org/10.1016/j.geotexmem.2009.03.006
25. Ekanayake SD, Liyanapathirana DS (2014) Leo C.J. Attenuation of ground vibrations using in-filled wave barriers. Soil Dyn Earthq Eng 67:290–300. https://doi.org/10.1016/j.soildyn.2014.10.004
26. Baker J (1994) An experimental study on vibration screening by in-filled trench barriers. MS thesis, State University of New York, Buffalo, USA.
27. Ahmad S, Baker J, Li J (1995) Experimental and numerical investigation on vibration screening by in-filled trenches. In: Proceedings of third international conference on recent advances in geotechnical earthquake engineering and soil dynamics, vol. II, Missouri, p. 757–62
28. Ahmad S, Al-Hussaini TM (1991) Simplified design for vibration screening by open and in-filled trenches. J Geotech Eng 117(1):67–88. https://doi.org/10.1061/(ASCE)0733-9410(1991)117:1(67)
29. Herbut A (2021) Wave generator as an alternative for classic and innovative wave transmission path vibration mitigation techniques. PLoS ONE 16(6):e0252088. https://doi.org/10.1371/journal.pone.0252088
30. Haupt WA (1977) Isolation of vibrations by concrete core walls. In: Proceedings of the ninth international conference on soil mechanics and foundation engineering, vol. 2, Tokyo, Japan, p. 251–56
31. El Naggar MH, Chehab AG (2005) Vibration barriers for shock-producing equipment. Can Geotech J 42:297–306. https://doi.org/10.1139/t04-067
32. Beskos DE, Dasgupta G, Vardoulakis IG (1986) Vibration isolation using open or filled trenches Part 1: 2-D homogeneous soil. Comput Mech 1(1):43–63. https://doi.org/10.1007/BF00298637

33. Ahmad S, Al-Hussaini TM, Fishman KL (1996) Investigation on active isolation of machine foundations by open trenches. J Geotech Eng 122:454–461. https://doi.org/10.1061/(ASCE)0733-9410(1996)122:6(454)
34. Al-Hussaini TM, Ahmad S (1991) Design of wave barriers for reduction of horizontal ground vibration. J Geotech Eng 117:616–636. https://doi.org/10.1061/(ASCE)0733-9410(1991)117:4(616)
35. Al-Hussaini TM, Ahmad S (1996) Active isolation of machine foundations by in-filled trench barriers. J Geotech Eng 122:288–294. https://doi.org/10.1061/(ASCE)0733-9410(1996)122:4(288)
36. Al-Hussaini TM, Ahmad S, Baker JM (2000) Numerical and experimental studies on vibration screening by open and in-filled trench barriers. In: Chouw, Schmid (eds) Proceedings of the international workshop on wave propagation, moving load and vibration reduction (wave 2000). Bochum, Rotterdam, Balkema, pp 241–250
37. Saikia A (2016) Active vibration isolation by open and in-filled trenches: a comparative study. ADBU-J Eng Technol 4(1):146
38. Saikia A (2015\2016) Numerical investigation on vibration isolation by softer in-filled trench barriers. J Geo Eng Sci 3:31–42. https://doi.org/10.3233/JGS-150034
39. Bose T, Choudhury D, Sprengel J, Ziegler M (2018) Efficiency of open and infill trenches in mitigating ground-borne vibrations. J Geotech Geoenviron Eng. https://doi.org/10.1061/(ASCE)GT.1943-5606.0001915
40. Yao J, Zhao R, Zhanga N, Yang D (2019) Vibration isolation effect study of in-filled trench barriers to train-induced environmental vibrations. Soil Dyn Earthq Eng 125:105741. https://doi.org/10.1016/j.soildyn.2019.105741
41. Qiu B (2015) Numerical study on vibration isolation by wave barrier and protection of existing tunnel under explosions; Civil Engineering. INSA deLyon, 2014.English.NNT:2014ISAL0011. tel-01127493.
42. Abbaszadeh Shahri A, PashamohammadiAsheghi FR, Abbaszadeh Shahri H (2021) Automated intelligent hybrid computing schemes to predict blasting induced ground vibration. Eng Comput. https://doi.org/10.1007/s00366-021-01444-1
43. Abbaszadeh Shahri A, Asheghi R (2018) Optimized developed artificial neural network-based models to predict the blast-induced ground vibration. Innov Infrastruct Solut 3:34. https://doi.org/10.1007/s41062-018-0137-4
44. Nguyen H, Bui XN, Tran QH, Mai NL (2019) A new soft computing model for estimating and controlling blast-produced ground vibration based on Hierarchical K-means clustering and Cubist algorithms. Appl Soft Comput J. https://doi.org/10.1016/j.asoc.2019.01.042
45. Vahidipour A, Ghanbari A, Hamidi A (2016) Experimental study of dynamic compaction for sand soils adjacent to the slope. Ground Improv 169(2):79–89. https://doi.org/10.1680/grim.14.00007
46. Mirzamomen A, Hamidi A, Ghanbari A (2019) Impact of model scale on the results of dynamic compaction adjacent to the sandy slopes. Ground Improv 172(2):65–75. https://doi.org/10.1680/jgrim.17.00022
47. Lukas RG (1986) Dynamic compaction for highway construction. Federal Highway Administration. Washington DC, USA. Vol. 1, Design and Construction Guidelines, Report No. FHWA/RD-86/133.
48. Mayne PW, Jones JS, Dumas JC (1984) Ground response to dynamic compaction. J Geotech Eng 110(6):757–771. https://doi.org/10.1061/(ASCE)0733-9410(1984)110:6(757)
49. Brule S, Javelaud EH, Enoch S, Guenneau S (2014) Experiments on seismic metamaterials: molding surface waves. Phys Rev Lett 112:133901
50. Chen Y, Qian F, Scarpa F, Zuo L, Zhuang X (2019) Harnessing multi-layered soil to design seismic metamaterials with ultralow frequency band gaps. Mater Des 175:107813. https://doi.org/10.1016/j.matdes.2019.107813
51. Miniaci M et al (2017) Proof of concept for an ultrasensitive technique to detect and localize sources of elastic nonlinearity using phononic crystals. Phys Rev Lett 118:214301. https://doi.org/10.1103/PhysRevLett.118.214301
52. Achaoui Y et al (2017) Clamped seismic metamaterials: ultra-low frequency stop bands. New J Phys 19:063022. https://doi.org/10.1088/1367-2630/aa6e21
53. Casablanca O et al (2018) Seismic isolation of buildings using composite foundations based on metamaterials. J Appl Phys 123:174903. https://doi.org/10.1063/1.5018005
54. Du Q et al (2018) H-fractal seismic metamaterial with broadband low-frequency bandgaps. J Appl Phys 51:105104. https://doi.org/10.1088/1361-6463/aaaac0
55. Oudich M et al (2018) Rayleigh waves in phononic crystal made of multilayered pillars: confined modes, fano resonances, and acoustically induced transparency. Phys Rev Appl. https://doi.org/10.1103/PhysRevApplied.9.034013
56. Oudich M et al (2017) Phononic crystal made of multilayered ridges on a substrate for Rayleigh waves manipulation. Crystals 7(12):372. https://doi.org/10.3390/cryst7120372
57. Lim CW, Reddy JM (2019) Built-up structural steel sections as seismic metamaterials for surface wave attenuation with low frequency wide bandgap in layered soil medium. Eng Struct 188:440–451. https://doi.org/10.1016/j.engstruct.2019.03.046
58. Palermo A, Vitali M, Marzani A (2018) Metabarriers with multi-mass locally resonating units for broad band Rayleigh waves attenuation. Soil Dyn Earthq Eng 113:265–277. https://doi.org/10.1016/j.soildyn.2018.05.035
59. Maleki M, Khodakarami M (2017) Feasibility analysis of using metasoil scatterers on the attenuation of seismic amplification in a site with triangular hill due to sv-waves. Soil Dyn Earthq Eng 100:169–182. https://doi.org/10.1016/j.soildyn.2017.05.036
60. Wen Huang H, Zhang B, Wang J, Menq FY, Nakshatrala KB, Mo YL, Stokoe KH (2021) Experimental study on wave isolation performance of periodic barriers. Soil Dyn Earthq Eng. https://doi.org/10.1016/j.soildyn.2021.106602
61. Abedini F, Rafiee-Dehkharghani R, Laknejadi K (2022) Mitigation of vibration caused by dynamic compaction considering soil non-linearity. Int J Civil Eng 20:809–826. https://doi.org/10.1007/s40999-022-00700-9